Evolution of South Atlantic density and chemical stratification across the last deglaciation

J. Roberts[a,b] *, J. Gottschalk[a], L. C. Skinner[a], V. L. Peck[b], S. Kender[c,d], H. Elderfield[a], C. Waelbroeck[e], N. Vázquez Riveiros[e], D. A. Hodell[a]

[a] Godwin Laboratory for Palaeoclimate Research, Department of Earth Sciences, University of Cambridge, Downing Street, Cambridge, CB2 3EQ; [b] British Antarctic Survey, High Cross, Madingley Road, Cambridge, CB3 0ET; [c] Centre for Environmental Geochemistry, School of Geography, University of Nottingham, Nottingham, NG7 2RD; [d] British Geological Survey, Nicker Hill, Keyworth, Nottingham, NG12 5GG; [e] Laboratoire des Sciences du Climat et de l' Environnement, Domaine du CNRS, 91198 Gif-sur-Yvette, France

Explanations of the glacial-interglacial variations in atmospheric pCO_2 invoke a significant role for the deep ocean in the storage of CO_2. Deep ocean density stratification has been proposed as a mechanism to promote the storage of CO_2 in the deep ocean during glacial times. A wealth of proxy data supports the presence of a "chemical divide" between intermediate and deep water in the glacial Atlantic Ocean, which indirectly points to an increase in deep ocean density stratification. However, direct observational evidence of changes in the primary controls of ocean density stratification, i.e. temperature and salinity, remain scarce. Here, we use Mg/Ca-derived seawater temperature and salinity estimates determined from temperature-corrected $\delta^{18}O$ measurements on the benthic foraminifer *Uvigerina spp.* from deep and intermediate water-depth marine sediment cores to reconstruct the changes in density of sub-Antarctic South Atlantic water masses over the last deglaciation (i.e. 22-2 ka before present). We find that a major breakdown in the physical density stratification significantly lags the breakdown of the deep-intermediate chemical divide, as indicated by the chemical tracers of benthic foraminifer $\delta^{13}C$ and foraminifer/coral ^{14}C. Our results indicate that chemical destratification likely resulted in the first rise in atmospheric pCO_2, whereas the density destratification of the deep South Atlantic lags the second rise in atmospheric pCO_2 during the late deglacial period. Our findings emphasise that the physical and chemical destratification of the ocean are not be as tightly coupled as generally assumed.

The last glacial termination was accompanied by an 80 ppm rise in atmospheric pCO_2 (1, 2), and it is widely believed that this increase in pCO_2 was driven by processes occurring within the Southern Ocean (3–5). These Southern Ocean processes are proposed to have released CO_2 from the deep ocean through a combination of decreased nutrient utilisation (6), increased vertical mixing (7) and increased air-sea gas exchange (8). Geochemical records show evidence for an 'old' (9) respired dissolved inorganic carbon pool in the glacial Southern Ocean below 2500m (10, 11) which became better ventilated over the course of the deglaciation (9, 12), supporting the idea that the deep ocean was isolated from the atmosphere during glacials. Over the deglacial period this chemical stratification between the deep ocean and the overlying intermediate ocean decreased, e.g.(11), implying a change in circulation or ventilation within the Southern Ocean which enabled CO_2 to be upwelled and outgassed to the atmosphere (7). The chemical destratification of the ocean has been attributed either to (i) an increase in air-sea gas exchange, through a decline in the extent of sea ice (8) and/or a decrease in surface ocean stratification (13); or (ii) a breakdown in the density stratification between the poorly-ventilated deep ocean and the better-ventilated water masses above (14). Evidence supporting either scenario remains elusive.

Pore-water profiles from deep ocean sediments have provided the first estimates of the density of the deep ocean during the Last Glacial Maximum (LGM) (15). These studies found that the glacial deep ocean was highly saline (~37 psu) and had an *in-situ* density that was 2 kg/m^3 denser than modern deep water. These studies lend support to the hypothesis that CO_2 storage within a highly stratified glacial ocean played a significant role in driving lower glacial atmospheric pCO_2. However, pore-water profiles only provide a 'snap-shot' of the physical properties of the deep ocean at the LGM, and do not provide information about the time-dependent changes in the density of deep water over the deglaciation. Thus, from these studies alone, it is impossible to assess whether the destratification of the deep ocean density gradients drove the atmospheric pCO_2 increase over the deglacial period.

Isotope-enabled intermediate complexity models have been used to suggest a mechanistic link between the physical (density) and chemical ($\delta^{13}C$) properties of the ocean over glacial-interglacial timescales (16, 17). These models suggest that deep ocean stratification, generated by the formation of dense brines during sea ice growth, is required to reconcile the spatial distribution of seawater $\delta^{13}C$. This result implies that a decrease in Antarctic sea ice, and therefore reduced brine formation, over the deglacial period will affect both the density of the deep ocean and its chemical properties synchronously. Testing this hypothesis of a mechanistic link between the physical and chemical properties of the ocean requires observational evidence of the density structure evolution of the Southern Ocean over the entire deglacial period.

Significance

The cause of the rise in atmospheric pCO_2 over the last deglaciation has been a puzzle since its discovery in the early 1980s. It is widely believed to be related to changes in carbon storage in the deep ocean, but the exact mechanisms responsible for releasing CO_2 from the deep ocean reservoir, including the role of ocean density stratification remains an open question. Here we reconstruct changes in the intermediate-deep density gradient in the South Atlantic across the last deglaciation and find evidence of an early deglacial chemical destratification and a late deglacial density destratification These results suggest that other mechanisms, besides deep ocean density destratification, were responsible for the ocean-atmosphere transfer of carbon over the deglacial period.

* email: jr451@cam.ac.uk

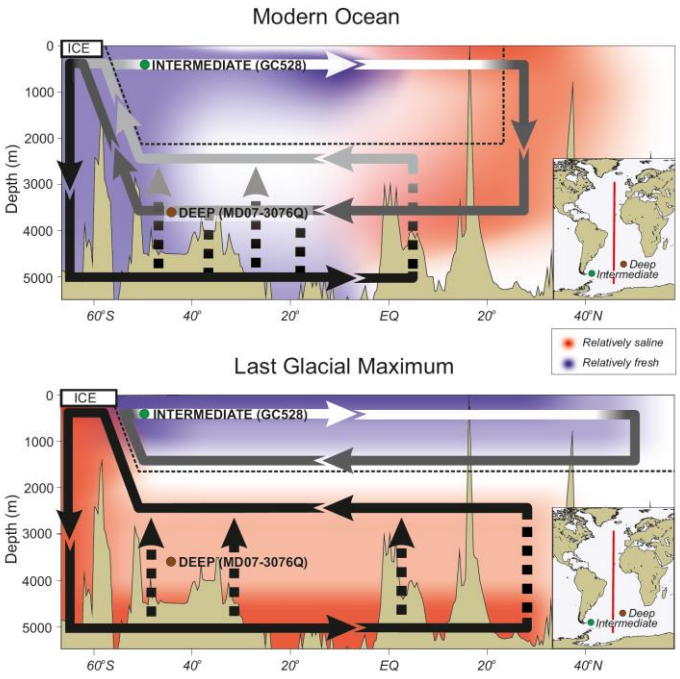

Figure 1: Location of intermediate (GC528) and deep (MD07-3076Q) sites. Site locations overlain on a schematic map of ocean circulation for (a) Modern and (b) Last Glacial Maximum, adapted from Ferrari et al., 2014 (41). The greyscale colours indicate the flow path of major water masses. Background colours indicate the relative salinity of water masses (blue – relatively fresh; red – relatively saline).

Here, we determine the deglacial evolution of the intermediate-deep density gradient in the high-latitude South Atlantic Ocean by generating temperature and salinity proxy records over the last 20 ka at the intermediate depth site of sediment core GC528 (598m; 58° 02.43'W, 53° 00.78'S) and the deep site of core MD07-3076Q (3770m; 14° 13.7'W, 44° 09.2'S) in the sub-Antarctic Atlantic [Figure 1]. We make the assumption that geochemical changes at a given depth occur synchronously within the South Atlantic (see Supporting Information). Combined Mg/Ca and $\delta^{18}O$ measurements on the benthic foraminifer *Uvigerina spp.* are used to estimate benthic seawater temperature (18) and to calculate the $\delta^{18}O$ of deep and intermediate water masses (hereafter referred to as δ_w). Temperature and δ_w (closely related to seawater salinity) are combined to produce a continuous record of the evolution of the density gradient in the South Atlantic over the last deglaciation (Methods). We compare the evolution of the density gradient with benthic $\delta^{13}C$ and ^{14}C records from the two sites in order to assess the hypothesis of a causal link between the physical and chemical properties of the deglacial ocean.

Deglacial changes in the physical properties of the South Atlantic

Although the deglacial decrease in *Uvigerina spp.* $\delta^{18}O$ is similar in both sites [Figure 2c], our Mg/Ca-derived temperature reconstructions [Figure 2b] suggest that the intermediate waters (GC528) were in fact cooler than the deep water (MD07-3076Q) for the majority of the glacial termination. This temperature inversion between the intermediate and deep sub-Antarctic reverses during the Early Holocene, from 9 ka onwards. It is physically impossible for cold intermediate water to overlie warmer deep water (even accounting for the effect of adiabatic decompression) and remain dynamically stable unless these differences are compensated by salinity.

We use the Mg/Ca-derived benthic temperatures and global sea level records (19) to deconvolve $\delta^{18}O$ of foraminiferal calcite [Figure 2c] into its principal components (20), i.e. temperature and δ_w [Methods]. In order to extract the salinity component from δ_w (21), we express δ_w as an offset from the contemporaneous 'global mean' δ_w, hereafter referred to as $\delta_{w\text{-}ice}$ [Figure 2d], by

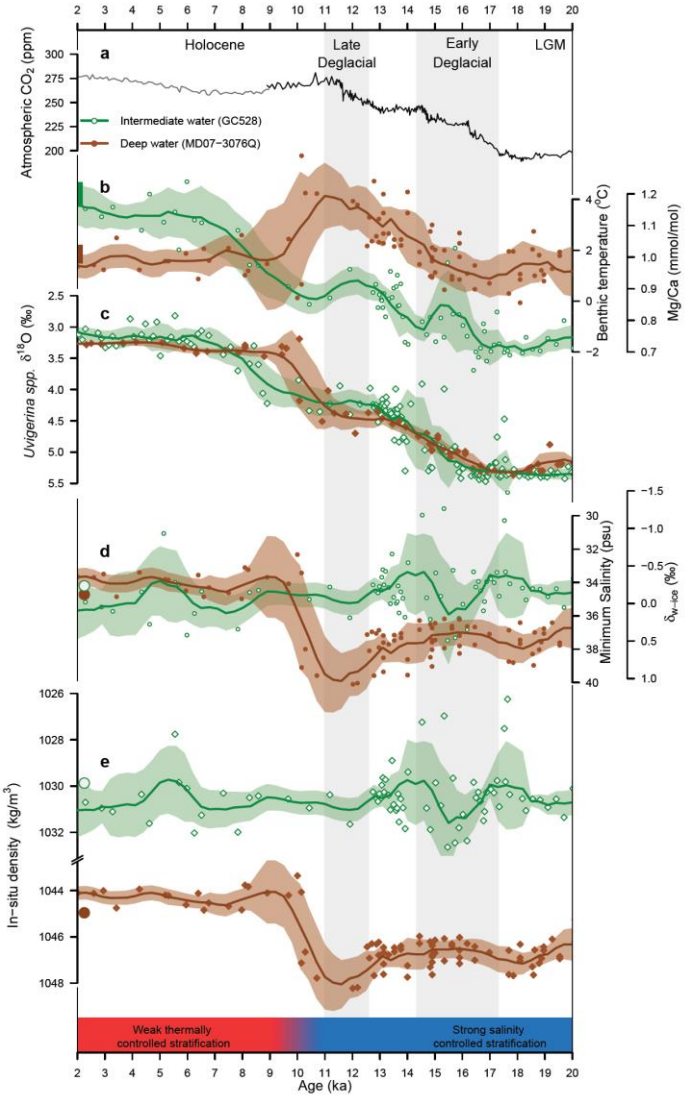

Figure 2: Deglacial records from intermediate (GC528) and deep (MD07-3076Q) water. a, Atmospheric CO_2 (WAIS Divide (50) – black; EDC (51) - grey); **b,** Mg/Ca-derived benthic temperatures for the intermediate site (GC528; green, open symbols) and the deep site (MD07-3076Q; brown, closed symbols). Thick bars at the start of each timeseries show modern temperature range; **c,** Foraminiferal $\delta^{18}O$ for the same sites as in b; **d,** $\delta^{18}O$ offset from contemporaneous 'global mean' $\delta^{18}O$ ($\delta_{w\text{-}ice}$) for the same sites as in b. Large circles at the start of each timeseries show modern salinity at each core site; **e,** *In-situ* density of the intermediate site (GC528) and the deep site (MD07-3076Q). Modern *in-situ* density shown by large circle at the start of each timeseries. The 1.5kyr spline and 1σ confidence interval for each plot shown as solid line and polygon respectively.

subtracting the isotopic effect of melting continental ice using global sea level records (19). The isotopic effect of melting ice will have spatial and temporal variations which are masked in our subtraction of a 'global mean' δ_w, however, without transient tracer models to prescribe a regional 'ice volume effect', the offset from the contemporaneous global mean δ_w remains the best approximation of ice sheet melt-derived $\delta^{18}O$ changes in the South Atlantic. Salinity is calculated from $\delta_{w\text{-}ice}$ assuming that the modern relationship between salinity and δ_w for the Southern Ocean (21) holds over the deglacial period. Recent isotope-enabled fully coupled GCM experiments have suggested that the salinity-δ_w relationship in the South Atlantic is more temporally constant than in other ocean basins (22) ruling out significant biases in our inferred salinity estimates due to potential variations in the salinity- δ_w relationship. However, brine rejection during the formation of sea ice increases salinity without fractionating oxygen isotopes; therefore, we suggest that salinity values derived from $\delta_{w\text{-}ice}$ are minimum estimates.

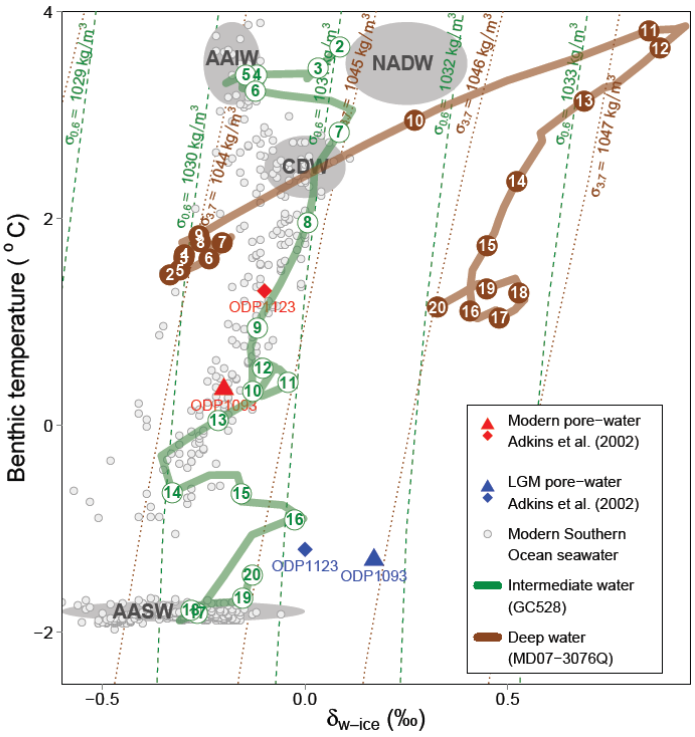

Figure 3: Temperature and $\delta^{18}O$ offset from contemporaneous 'global mean' $\delta^{18}O$ ($\delta_{w\text{-}ice}$) evolution of Southern Ocean Water masses over the last deglaciation. Composite plot of intermediate water (GC528 – green, open symbols) and deep water (MD07-3076Q – brown, closed symbols) evolution, ages in ka shown in circles. *In-situ* density isopycnals of GC528 (green dashed lines) and MD07-3076Q (brown dotted lines) shown in background. Grey dots represent modern seawater T-$\delta_{w\text{-}ice}$ (30), AAIW -Antarctic Intermediate Water; AASW - Antarctic Surface Water; CDW - Circumpolar Deep Water; NADW – North Atlantic Deep Water.

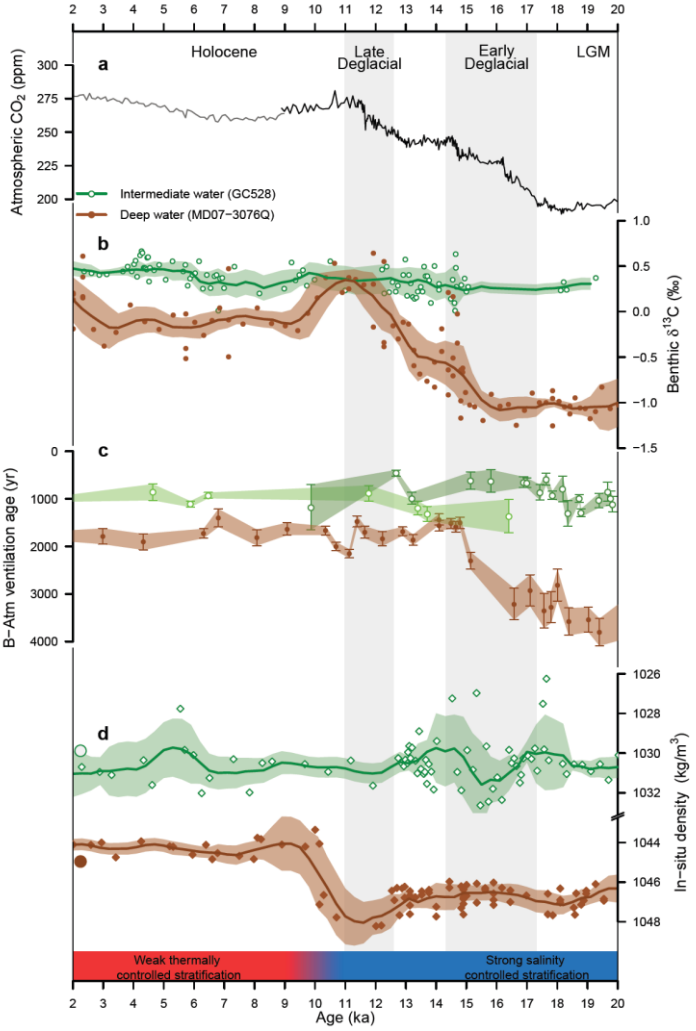

Figure 4: Comparison between the intermediate-deep density gradient and the chemical gradient. a, Atmospheric CO_2 (WAIS Divide (50) – black; EDC (51) - grey); **b,** Chemical properties, $\delta^{13}C$ of foraminiferal calcite, for intermediate (GC528 – green, open symbols) and deep water (MD07-3076Q – brown, closed symbols); **c,** Apparent water mass ventilation age (B-Atm), intermediate water (Burdwood Bank – pale green, open symbols (12); Chile Margin – dark green, open symbols (35)) and deep water (MD07-3076Q – brown, closed symbols (9)); **d** *In-situ* density of the intermediate site (GC528) and the deep site (MD07-3076Q).

The difference in intermediate water salinity between the LGM and the Holocene is small (Figure 2d) as most of the deglacial $\delta^{18}O$ *Uvigerina spp.* variation can be accounted for by warming. By contrast, the deep water site (MD07-3076Q) was relatively saline (36-37 psu) during the glacial period and salinity decreased by 3-4 psu during the late deglacial (12-9 ka).

Using the Mg/Ca-derived benthic temperatures and our estimates of minimum salinity we calculate the *in-situ* density of the intermediate and deep site according to the equation of state (23) (Figure 2e). We find good agreement between our density estimates for the Holocene and modern South Atlantic density measurements (Figure 2e). The deglacial density reconstructions indicate the presence of a strong density gradient between intermediate and deep water for the glacial and much of the deglacial period. This density gradient decreases dramatically from 12 ka, and by 10 ka the deep ocean is 2 kg/m^3 less dense than at the LGM. Our Mg/Ca-$\delta^{18}O$ derived deep ocean LGM salinities are broadly consistent with previous porewater based estimates (15) (Figure 3). Although both reconstructions carry substantial uncertainty (24) (Supplementary material), the convergence of two independent methods strengthens our confidence in both approaches. Prior to 12 ka the high salinity of the deep water site implies a strong density gradient, despite the temperature inversion of cool intermediate waters overlying warmer deep water. After 10 ka the salinity stratification has broken down, and a weaker density gradient is maintained by the temperature difference between intermediate and deep water. Provided the assumption of zonal seawater density continuity across the sub-Antarctic Atlantic holds true, our findings signal a significant mode switch in the primary physical parameters that govern ocean density stratification in the southern high-latitudes through the last deglaciation.

Processes controlling the physical properties of water masses over the deglaciation

To determine the factors affecting the variability in the physical properties of deep and intermediate water masses over the deglaciation, we compare glacial water mass temperature and $\delta_{w\text{-}ice}$ properties with those of water masses present in the Southern Ocean today (Figure 3). Comparison of intermediate LGM temperature-$\delta_{w\text{-}ice}$ with modern measurements of seawater temperature and δ_w suggests that LGM intermediate water was analogous to modern Antarctic Surface Water (AASW), which is characterised by near freezing temperatures (Figure 3). Such low temperatures suggest that the source location of intermediate water was strongly influenced by sea ice (which forms from seawater with a temperature of -2°C). Glacial sea ice reconstructions using diatom transfer functions (25, 26) predict that winter sea ice could have extended as far north as 57°S at this longitude. We therefore suggest that glacial intermediate water masses at GC528 reflect the cold and fresh signature of surface waters close to the winter sea ice edge that is influenced by seasonal sea ice meltwater. This is in stark contrast to modern intermediate water at GC528,

which is strongly influenced by a modified component of upwelled Circumpolar Deep Water (27) (Figure 3).

The processes controlling the benthic temperature of the deep site are more complex. Deep water formed close to the sea ice margin can only gain heat in two ways; (i) through mixing with other, warmer water masses, and (ii) through the accumulation of geothermal heat in the deep sea. The most probable warm water masses that can mix with sinking southern-sourced waters during the LGM are Drake Passage through flow waters from the Pacific. Although it has been shown that Pacific deep water was not significantly warmer than freezing (18, 28), it remains to be determined whether Pacific intermediate waters were significantly warmer and had an influence on southern-sourced deep water in the Atlantic. Alternatively, the source of warmth in the deep South Atlantic may be derived from the accumulation of geothermal heat, assuming that the deep ocean is stagnant and cannot lose heat to the surface (29). It has been shown by a conceptual model that it would take 10kyrs to heat 2km of seawater by $2^{o}C$, based on a heat flux of $500mW/m^2$ (29). Both of these processes may have potentially accounted for the observed warmth of the salty LGM deep water in the South Atlantic. However, an analysis of whether a completely stagnant and isolated deep water pool is physically possible or whether it was significantly influenced by Pacific inflow waters goes beyond the scope of this study.

The deglacial evolution of deep water temperature and $\delta_{w\text{-}ice}$ (Figure 3) can be understood by invoking a combination of (i) changes in the northern versus southern mixing ratio and (ii) changes in the end-member $\delta^{18}O$ of Antarctic Bottom Water (AABW). In the modern Atlantic Ocean, saline North Atlantic Deep Water (NADW) overlies fresh AABW (Figure1). The high $\delta^{18}O$ signature of NADW reflects high rates of evaporation at the surface, whereas the $\delta^{18}O$ of AABW is comparatively more negative (30). The warming and increase in $\delta_{w\text{-}ice}$ over much of the deglaciation (16-12 ka) may indicate a greater proportion of northern-sourced water at MD07-3076Q. This is supported by benthic foraminifer ε_{Nd} data that suggests an increasing contribution of northern-sourced water in the South Atlantic throughout the deglaciation (31). The late deglacial change in deep water $\delta_{w\text{-}ice}$ to isotopically lighter values after 12ka is likely driven by a change in the mode of AABW formation. The two different modes of southern-sourced deep water formation, i.e. brine rejection during sea ice formation and super-cooling of Ice Shelf Water (ISW) beneath the Antarctic ice shelves (32), impart very different signals on $\delta_{w\text{-}ice}$. Brines have a $\delta^{18}O$ signature close to surface water values (~0‰ in the Southern Ocean), whereas ISW has a negative $\delta^{18}O$ signature reflecting incorporation of overlying ice shelf meltwater. We would argue that the marked decrease in the $\delta_{w\text{-}ice}$ of deep water at 12 ka is related to an increasing contribution of ISW constituting AABW. This change may be associated with a retreat in the grounding line of Weddell Sea ice shelves and an intrusion of relatively warm modified northern-sourced water under the ice shelves, further melting the marine-terminating ice sheets around Antarctica (33). In summary, the modes of intermediate and deep water formation have a profound impact on the density structure of the sub-Antarctic ocean.

The link between the physical and chemical properties of the South Atlantic and atmospheric pCO_2

In order to assess the hypothesis of a causal link between the physical and chemical properties of the ocean, we compare the timing of changes in the breakdown of the density gradient with changes in benthic foraminifer $\delta^{13}C$ and foraminifer/coral benthic-atmospheric ^{14}C ages at both core locations (Figure 4). Benthic foraminifer $\delta^{13}C$ at the intermediate water site (GC528) was more positive than the $\delta^{13}C$ of the deep site (MD07-3076Q; (34)) at the LGM (Figure 4b). This large $\delta^{13}C$ gradient breaks down over the deglaciation (15-10 ka) resulting in relatively homogeneous $\delta^{13}C$ values at both sites during the Holocene. Foraminifer/coral benthic-atmospheric ^{14}C age offsets between intermediate (Burdwood Bank (12), Chile Margin (35)) and deep water (MD07-3076Q (9)) are broadly consistent with the $\delta^{13}C$ record (Figure 4c). These two records provide strong support for glacial chemical stratification, which subsequently breaks down relatively early in the deglaciation.

Comparison of the deglacial density records (Figure 4d) and the chemical $\delta^{13}C$ and ^{14}C records (Figure 4b-c), shows a marked difference in the timing of the breakdown of density and chemical gradients. In the deep site, both the $\delta^{13}C$ and ^{14}C records begin to change in early in the deglaciation (17-15 ka), and in the case of the foraminiferal ^{14}C record, these early decreases in the benthic-atmospheric ^{14}C age have been linked to a synchronous rise in atmospheric CO_2 (9). However, there is no concomitant change in the intermediate-deep density gradient at this time (Figure 4d). The onset of the physical destratification occurs during the Early Holocene (~10 ka), and appears to lag the late deglacial rise in atmospheric pCO_2. Our proxy records suggest that (i) changes in ocean chemistry in the South Atlantic occur without large-scale reorganisation of the ocean's density structure, challenging the propositions of a close coupling between physical and chemical ocean stratification as suggested by intermediate complexity models (17), and (ii) the density destratification of the South Atlantic could only have impacted atmospheric pCO_2 during the late deglaciation.

CO_2 stored in the deep ocean can be impeded from being released back to the atmosphere by two physical processes; (i) via an increased residence time of deep water masses in the ocean interior, through an increase in deep ocean stratification acting as a lid to deep carbon (7); or (ii) reduced efficiency of air-sea gas exchange in the regions of deep mixing and upwelling (8). We suggest that during the LGM, both of these processes will have contributed to lower atmospheric pCO_2, owing to increased density stratification in the Southern Ocean and because permanent sea ice (8) and/or shallow stratification (13, 36) acted as a barrier preventing CO_2 from escaping the surface of the Southern Ocean. Indeed, it is plausible that the retreat of sea ice during the early deglaciation (26, 37) effectively removed a barrier to air-sea exchange, and thus contributed to the increase in atmospheric pCO_2 through enhanced ventilation of the deep overturning cell (9, 31). The hypothesis of an early retreat in the extent of Antarctic sea ice is also supported by the warming trend observed in GC528 at 17-15ka [Figure 2b]. However the retreat of sea ice cover in the South Atlantic might not have had a significant effect on the density difference between the intermediate and deep overturning cells because the mode of deep water formation did not change, which is controlled by the position of the grounded ice sheet relative to the continental shelf break. Although the geological evidence for the position of the grounding line in the Weddell Sea is inconsistent (38), there is indication that, at least around the Antarctic Peninsula, the grounding line retreat occurred late in the deglaciation (39, 40). Thus the glacial brine-dominated mode of southern-sourced deep water formation may have persisted until as late as 10 ka. In summary, we argue that changes in the extent of permanent sea ice may occur earlier than changes in the maximum position of the grounded icesheets, thus it is possible to ventilate the deep ocean without decreasing its density.

Over the deglacial period (17-11ka), increasing deep ocean temperatures [Figure 2b] coupled with a 0.6‰ increase in benthic foraminifer $\delta^{13}C$ (34) (Figure 4b) is indicative of a greater proportion of northern-sourced water in the deep South Atlantic.

The impinging of warm modified northern-sourced water on the Antarctic continental shelf has been suggested as a possible mechanism (33) which could melt back the grounded ice sheets in the Weddell Sea, freeing shelf space for the formation of ISW, resulting in the observed decrease in deep ocean density stratification at 10ka. Whilst a decrease in the density of deep water has been invoked to explain the deglacial rise in atmospheric pCO_2, via associated changes in the rate of diapycnal mixing and the vertical position of the isopycnal separating the two overturning branches of circulation (16, 17, 41), we suggest that its impact is relatively minor compared to the impact of changes in the rate of air-sea gas exchange in the Southern Ocean. However, it should be noted that vertical shifts in the position of the main pycnocline (41) cannot be resolved in this study, thus it remains to be determined whether these changes play a more important role in regulating atmospheric CO_2.

Although density destratification of the South Atlantic does not appear to play a leading role in regulating atmospheric pCO_2 we propose that density destratification may have been instead important in 'locking in' the incipient transition to an interglacial climate state. Prior to the destratification event, the ocean was able to return to its 'glacial regime' following a transient perturbation; but not afterwards. We suggest that the density destratification of the South Atlantic, initiated by a change in mode of formation of deep water, acted as a 'flip switch', eliminating the ocean's ability to re-stock its CO_2 inventory at the expense of the atmosphere, and thus forcing climate to switch to an interglacial state. Longer records of the density gradient within the Southern Ocean are required to test this hypothesis.

Conclusion

This study provides the first deglacial record of density changes in the deep and intermediate South Atlantic spanning the last deglaciation. We find that the intermediate ocean was significantly colder than deep waters at the LGM, and this temperature inversion requires that ocean stability is maintained by salinity gradients. We suggest that the physical properties of the glacial South Atlantic were regulated by an increase in Antarctic sea ice extent, which resulted in colder surface waters in the sub-Antarctic, but also led to deep waters being primarily formed through the creation of brines as opposed to super-cooling of ISW. Over the deglaciation, intermediate water warmed in response to a retreat in the Antarctic sea ice margin, and the deep South Atlantic started to reflect both a greater proportion of northern-sourced water but also isotopically lighter AABW from the incorporation of Antarctic ice sheet meltwater. A rapid change in the dominant mode of deep water formation at the onset of the Holocene, from brines to super-cooled ISW, likely resulted in the density destratification of the intermediate-deep ocean during the late deglacial period.

Our density records also enable us to address the question of whether deglacial changes in ocean chemistry are driven by a breakdown in the deep ocean density stratification. We find that the greatest intermediate-deep change in benthic foraminifer $\delta^{13}C$ and foraminifer/coral ^{14}C occurs prior to the density destratification. We suggest that this chemical destratification was driven by an increase in air-sea gas exchange which ventilates the deep overturning cell without affecting its density. The late deglacial breakdown in the density gradient of the South Atlantic occurs at the onset of the Holocene, suggesting deep ocean density destratification did not play a leading role in driving the deglacial rise in atmospheric pCO_2. The difference in the timing of the breakdown of the intermediate-deep chemical gradient compared to the breakdown of the intermediate-deep physical density gradient suggests that chemical and physical stratification is not be as tightly coupled as previously inferred. This also raises the interesting possibility that the density destratification of the South Atlantic, induced by a change in the mode of deep water formation, could act as the 'flip switch' resulting in the transition to a full interglacial state.

Methods

Materials

Core GC528 [53.01°S, 58.04°W, 598mbsl] was collected on the cruise JR244 of the RRS *James Clark Ross*. Located on the Falkland Plateau, this core is situated close to the main inflow of AAIW into the Atlantic basin.

Core MD07-3076Q [44° 09.2'S 14° 13.7'W, 3770mbsl] was retrieved from the eastern flank of the mid-ocean ridge. The age model is based on reservoir-age corrected radiocarbon measurements on monospecific planktonic foraminifera and is described fully in ref. (36).

Age model (GC528)

The age model for GC528 (Supporting Information) was generated using 25 radiocarbon dates of monospecific samples of *Uvigerina bifurcata* (>125µm size fraction, 2-6mg), which were graphitised in the Godwin Laboratory for Palaeoclimate Research, University of Cambridge (hereafter, GLPR) using the hydrogen and iron catalyst method (42) and subsequently analysed at the ^{14}Chrono Centre at the University of Belfast by Accelerator Mass Spectrometry. 5 of the 25 samples were graphitised and analysed by BetaAnalytic, no inter-lab offset between samples was found. Carbon-14 ages were calibrated using *Bacon* age-modelling software (43) with the Marine13 dataset(44). Reservoir age constraints were taken from paired U-Th/^{14}C ages in corals(12) after 16ka, prior to 16ka a constant reservoir age of 1.36±0.4kyr (the age of the oldest U-Th/^{14}C dated coral analysed by Burke et al. (12)) was applied downcore.

Sample Preparation

In GC528, samples of *Uvigerina spp.* (212-315µm size fraction) were hand-picked, cleaned using the methodology of ref. (45) and split, with ~100ug used for oxygen and carbon isotope and ~400ug for trace element geochemistry were analysed at the GLPR.

In MD07-3076Q, samples of *Uvigerina spp.* (212-315µm size fraction) were hand-picked and ~3 whole specimens were used for stable isotope analysis, and 10-15 whole specimens were cleaned for Mg/Ca analysis using the methodology of ref. (45).

Oxygen and stable carbon isotopes

Stable isotopes from GC528 were analysed using a Multicarb preparation system coupled to a VG SIRA Mass Spectrometer in the GLPR. Measurements of $\delta^{18}O$ and $\delta^{13}C$ were determined relative to the Vienna Peedee Belemnite (VPDB) standard with an analytical precision of ±0.08‰ for $\delta^{18}O$ and ±0.06‰ for $\delta^{13}C$. $\delta^{18}O$ was measured on *Uvigerina spp.* and $\delta^{13}C$ was measured on *Oridorsalis umbonatus* and corrected to equilibrium calcite by +1.0‰ (46). Although *O.umbonatus* is a shallow infaunal species, the $\delta^{13}C$ *O.umbonatus* correlation with coral ^{14}C trends from intermediate water (12, 35) suggests that there has been no bias in the overprinting of bottom water $\delta^{13}C_{DIC}$ by porewaters. Stable isotopes from MD07-3076Q were analysed at the Laboratoire des Sciences du Climat et de l'Environnement, Gif sur Yvette. The mean external reproducibility of the carbonate standard is ±0.05‰ for $\delta^{18}O$ and ±0.03‰ for $\delta^{13}C$. $\delta^{18}O$ was measured on *Uvigerina spp.* and $\delta^{13}C$ was measured on *Cibicides kullenbergi* (34).

Trace metal analysis

Mg/Ca elemental ratios were determined by Inductively Coupled Plasma–Optical Emission Spectroscopy (47). Long-term instrumental precision of element ratio data, determined by replicate analyses of a standard solution was ± 0.46%, translating into an uncertainty of 0.06°C.

Bottom water carbonate ion concentration has been previously suggested (48) to affect Mg/Ca values in some benthic foraminifera species. Deglacial variation in carbonate ion concentration may exert an effect on Mg/Ca which is unrelated to changes in bottom water temperature, particularly at the deep site (MD07-3076Q) where carbonate ion concentrations are lower. However, recent studies (e.g. 18) show

that *Uvigerina spp.* Mg/Ca (in particular) is very insensitive to changes in the carbonate ion concentration.

Mg/Ca-derived benthic temperatures

Mg/Ca values were converted into benthic temperatures using the new calibration curve (Supplementary Information):

$Mg/Ca = (0.0915\pm0.005)*T + (0.843\pm0.035)$ $R^2 = 0.92$

1σ uncertainty in the temperature estimate of each sample is ±0.7°C (Supplementary Information).

Seawater $\delta^{18}O$ offset from the contemporaneous 'global mean' seawater $\delta^{18}O$ ($\delta_{w\text{-}ice}$)

Seawater $\delta^{18}O$ (δ_w) is calculated from the Mg/Ca-derived benthic temperature and the $\delta^{18}O$ of foraminiferal calcite using the linear form of the palaeo-temperature equation of ref. (20):

$T = 16.9 - 4.0*(\delta_c - \delta_w)$

This calibration produces good agreement between modern measurements of δ_w and the calculated core top δ_w.

To make a comparison to modern seawater values, the contemporaneous 'global mean' seawater $\delta^{18}O$, sometimes referred to as 'ice-volume effect', was removed assuming a linear relationship (21) between sea level (19) and $\delta^{18}O$ of seawater. Site-specific deviations from the global mean that would result in a synchronous breakdown of the physical and chemical gradients in the South Atlantic require changes in δ_w in MD07-3076Q 5kyr earlier than the global mean, which is not supported by regional $\delta^{18}O$ stacks (49). 1σ uncertainty in $\delta_{w\text{-}ice}$ of each sample is ±0.35‰.

***In-situ* density of seawater (σ_θ)**

The modern linear relationship between salinity and $\delta_{w\text{-}ice}$ for the Southern Ocean (21) is assumed to hold across the deglacial period (Supporting Information). *In-situ* density was calculated from salinity and benthic temperature, using the equation of state (23).

Acknowledgements

We are grateful to I. Mather, J. Rolfe, F. Dewilde and G. Isguder for preparing and performing isotopic analyses, as well as C. Daunt, S. Souanef-Ureta and M. Greaves for technical assistance in performing trace element analysis. J.R. was funded jointly by the British Geological Survey/British Antarctic Survey (Natural Environment Research Council) and the University of Cambridge. J.G. was funded by the Gates Cambridge Trust. L.C.S. acknowledges support from the Royal Society and NERC grant NE/J010545/1. C.W. acknowledges support from the European Research Council grant ACCLIMATE/no 339108. This is LSCE contribution 5514. This work was funded (in part) by the European Research Council (ERC grant 2010-NEWLOG ADG-267931 HE). N.V.R. acknowledges support from EU RTN NICE (no. 36127). We thank the captain and crew of the RRS *James Clark Ross* for facilitating the collection of the marine sediment core GC528.

1. Delmas RJ, Ascencio J-M, Legrand M (1980) Polar ice evidence that atmospheric CO2 20,000 yr BP was 50% of present. *Nature* 284(5752):155–157.
2. Neftel A, Oeschger H, Schwander J, Stauffer B, Zumbrunn R (1982) Ice core sample measurements give atmospheric CO2 content during the past 40,000 yr. *Nature* 295(5846):220–223.
3. Knox F, McElroy MB (1984) Changes in Atmospheric CO2: Influence of the Marine Biota at High Latitude. *J Geophys Res* 89:4629–4637.
4. Siegenthaler U, Wenk T (1984) Rapid Atmospheric CO2 Variations and Ocean Circulation. *Nature* 308(5960):624–626.
5. Sarmiento JL, Toggweiler JR (1984) A new model for the role of the oceans in determining atmospheric PCO2. *Nature* 308(5960):621–624.
6. Martin JH (1990) Glacial-interglacial CO2 change: The Iron Hypothesis. *Paleoceanography* 5(1):1–13.
7. Toggweiler JR (1999) Variation of atmospheric CO2 by ventilation of the ocean's deepest water. *Paleoceanography* 14(5):571–588.
8. Stephens B, Keeling R (2000) The influence of Antarctic sea ice on glacial-interglacial CO2 variations. *Nature* 404(6774):171–174.
9. Skinner LC, Fallon S, Waelbroeck C, Michel E, Barker S (2010) Ventilation of the deep Southern Ocean and deglacial CO2 rise. *Science (80-)* 328(5982):1147–1151.
10. Boyle EA (1988) The role of vertical chemical fractionation in controlling late Quaternary atmospheric carbon dioxide. *J Geophys Res* 93(C12):15701–15714.
11. Hodell DA, Venz KA, Charles CD, Ninnemann US (2003) Pleistocene vertical carbon isotope and carbonate gradients in the South Atlantic sector of the Southern Ocean. *Geochemistry, Geophys Geosystems* 4(1):1–19.
12. Burke A, Robinson LF (2012) The Southern Ocean's role in carbon exchange during the last deglaciation. *Science* 335(6068):557–61.
13. Francois R, et al. (1997) Contribution of Southern Ocean surface-water stratification to low atmospheric CO2 concentrations during the last glacial period. *Nature* 389(6654):929–936.
14. Sigman DM, Hain MP, Haug GH (2010) The polar ocean and glacial cycles in atmospheric CO2 concentration. *Nature* 466(7302):47–55.
15. Adkins JF, McIntyre K, Schrag DP (2002) The salinity, temperature, and δ18O of the glacial deep ocean. *Science* 298(5599):1769–73.
16. Tagliabue A, et al. (2009) Quantifying the roles of ocean circulation and biogeochemistry in governing ocean carbon-13 and atmospheric carbon dioxide at the last glacial maximum. *Clim Past* 5(4):695–706.
17. Bouttes N, Paillard D, Roche DM (2010) Impact of brine-induced stratification on the glacial carbon cycle. *Clim Past* 6(5):575–589.
18. Elderfield H, et al. (2010) A record of bottom water temperature and seawater δ18O for the Southern Ocean over the past 440 kyr based on Mg/Ca of benthic foraminiferal Uvigerina spp. *Quat Sci Rev* 29(1-2):160–169.
19. Lambeck K, Rouby H, Purcell A, Sun Y, Sambridge M (2014) Sea level and global ice volumes from the Last Glacial Maximum to the Holocene. *Proc Natl Acad Sci U S A* 111(43):15296–15303.
20. Shackleton NJ (1974) Attainment of Isotopic Equilibrium Between Ocean Water and the Benthonic Foraminifera Genus Uvigerina: Isotopic Changes in the Ocean During the Last Glacial. 219:203–209.
21. LeGrande AN, Schmidt GA (2006) Global gridded data set of the oxygen isotopic composition in seawater. *Geophys Res Lett* 33(12):L12604.
22. Holloway MD, Sime LC, Singarayer JS, Tindall JC, Valdes PJ (2015) Reconstructing paleosalinity from δ18O: Coupled model simulations of the Last Glacial Maximum, Last Interglacial and Late Holocene. *Quat Sci Rev*.
23. Jackett DR, McDougall TJ, Feistel R, Wright DG, Griffies SM (2010) Algorithms for Density, Potential Temperature, Conservative Temperature, and the Freezing Temperature of Seawater. *J Atmos Ocean Technol.* 23:1709–1728.
24. Miller MD, Simons M, Adkins JF, Minson SE (2015) The Information Content of Pore Fluid δ 18 O and [Cl −]. *J Phys Oceanogr* 45(8):2070–2094.
25. Gersonde R, Crosta X, Abelmann A, Armand L (2005) Sea-surface temperature and sea ice distribution of the Southern Ocean at the EPILOG Last Glacial Maximum—a circum-Antarctic view based on siliceous microfossil records. *Quat Sci Rev* 24(7-9):869–896.
26. Allen CS, Pike J, Pudsey CJ (2011) Last glacial–interglacial sea-ice cover in the SW Atlantic and its potential role in global deglaciation. *Quat Sci Rev* 30(19-20):2446–2458.
27. Tomczak M, Godfrey JS (2001) Antarctic Oceanography. *Regional Oceanography: An Introduction*, pp 63–83.
28. Woodard SC, et al. (2014) Antarctic role in Northern Hemisphere glaciation. *Science* 346(6211):847–51.
29. Adkins JF, Ingersoll AP, Pasquero C (2005) Rapid climate change and conditional instability of the glacial deep ocean from the thermobaric effect and geothermal heating. *Quat Sci Rev* 24(5-6):581–594.
30. Meredith MP, et al. (1999) Distribution of oxygen isotopes in the water masses of Drake Passage and the South Atlantic. *J Geophys Res* 104(C9):20949–20962.
31. Skinner LC, et al. (2013) North Atlantic versus Southern Ocean contributions to a deglacial surge in deep ocean ventilation. *Geology* 41(6):667–670.
32. Krueger S, Leuschner DC, Ehrmann W, Schmiedl G, Mackensen A (2012) North Atlantic Deep Water and Antarctic Bottom Water variability during the last 200ka recorded in an abyssal sediment core off South Africa. *Glob Planet Change* 80-81:180–189.
33. Adkins JF (2013) The role of deep ocean circulation in setting glacial climates. *Paleoceanography* 28(3):539–561.
34. Waelbroeck C, et al. (2011) The timing of deglacial circulation changes in the Atlantic. *Paleoceanography* 26(3):PA3213.
35. De Pol-Holz R, Keigwin L, Southon J, Hebbeln D, Mohtadi M (2010) No signature of abyssal carbon in intermediate waters off Chile during deglaciation. *Nat Geosci* 3(3):192–195.

36. Gottschalk J, Skinner LC, Waelbroeck C (2015) Contribution of seasonal sub-Antarctic surface water variability to millennial-scale changes in atmospheric CO2 over the last deglaciation and Marine Isotope Stage 3. *Earth Planet Sci Lett* 411:87–99.
37. Collins LG, Pike J, Allen CS, Hodgson DA (2012) High-resolution reconstruction of southwest Atlantic sea-ice and its role in the carbon cycle during marine isotope stages 3 and 2. *Paleoceanography* 27(3):PA3217.
38. Hillenbrand C-D, et al. (2012) Grounding-line retreat of the West Antarctic Ice Sheet from inner Pine Island Bay. *Geology* 41(1):35–38.
39. Pudsey CJ, Murray JW, Appleby P, Evans J (2006) Ice shelf history from petrographic and foraminiferal evidence, Northeast Antarctic Peninsula. *Quat Sci Rev* 25(17-18):2357–2379.
40. Johnson JS, Bentley MJ, Roberts SJ, Binnie SA, Freeman SPHT (2011) Holocene deglacial history of the northeast Antarctic Peninsula – A review and new chronological constraints. *Quat Sci Rev* 30(27-28):3791–3802.
41. Ferrari R, et al. (2014) Antarctic sea ice control on ocean circulation in present and glacial climates. *Proc Natl Acad Sci U S A* 111(24):8753–8758.
42. Vogel JS, Southon JR, Nelson DE, Brown TA (1984) Performance of catalytically condensed carbon for use in accelerator mass spectrometry. *Nucl Instruments Methods Phys Res Sect B Beam Interact with Mater Atoms* 5(2):289–293.
43. Blaauw M, Christen JA (2011) Flexible paleoclimate age-depth models using an autoregressive gamma process. *Bayesian Anal* 6(3):457–474.
44. Reimer P, et al. (2013) IntCal13 and Marine13 Radiocarbon Age Calibration Curves 0–50,000 Years cal BP. *Radiocarbon* 55(4):1869–1887.
45. Barker S, Greaves M, Elderfield H (2003) A study of cleaning procedures used for foraminiferal Mg/Ca paleothermometry. *Geochemistry, Geophys Geosystems* 4(9):8407.
46. Woodruff F, Savin SM, Douglas RG (1980) Biological fractionation of oxygen and carbon isotopes by recent benthic foraminifera. *Mar Micropaleontol* 5:3–11.
47. Villiers S de, Greaves M, Elderfield H (2002) An intensity ratio calibration method for the accurate determination of Mg/Ca and Sr/Ca of marine carbonates by ICP-AES. *Geochemistry Geophys Geosystems* 3:1001.
48. Elderfield H, Yu J, Anand P, Kiefer T, Nyland B (2006) Calibrations for benthic foraminiferal Mg/Ca paleothermometry and the carbonate ion hypothesis. *Earth Planet Sci Lett* 250(3-4):633–649.
49. Stern J V., Lisiecki LE (2014) Termination 1 timing in radiocarbon-dated regional benthic δ 18 O stacks. *Paleoceanography* 29(12):1127–1142.
50. Marcott SA, et al. (2014) Centennial-scale changes in the global carbon cycle during the last deglaciation. *Nature* 514(7524):616–619.
51. Monnin E, et al. (2004) Evidence for substantial accumulation rate variability in Antarctica during the Holocene, through synchronization of CO2 in the Taylor Dome, Dome C and DML ice cores. *Earth Planet Sci Lett* 224(1-2):45–54.